Semiconductors, Vol. 35, No. 8, 2001, pp. 904–911. Translated from Fizika i Tekhnika Poluprovodnikov, Vol. 35, No. 8, 2001, pp. 941–947.

ELECTRONIC AND OPTICAL PROPERTIES OF SEMICONDUCTORS

The Role of Lead in Growing $Ga_{1-X}In_XAs_YSb_{1-Y}$ Solid Solutions by Liquid-Phase Epitaxy

T. I. Voronina, T. S. Lagunova, E. V. Kunitsyna, Ya. A. Parkhomenko, D. A. Vasyukov, and Yu. P. Yakovlev

Ioffe Physicotechnical Institute, Russian Academy of Sciences, Politekhnicheskaya ul. 26, St. Petersburg, 194021 Russia

Submitted December 27, 2000; accepted for publication February 15, 2001

Abstract—The electrical properties of $Ga_{1-X}In_XAs_YSb_{1-Y}$ (X = 0.14–0.27) solid solutions grown from a Pb-containing solution–melt were investigated for the first time. Three acceptor levels were found to exist, specifically, a shallow level with the activation energy $E_{A1} \approx 0.008$–0.015 eV, and two deep levels $E_{A2} \approx 0.024$–0.033 eV and $E_{A3} \approx 0.07$ eV. It is demonstrated that the use of Pb makes it possible to obtain undoped solid solutions with a low concentration of defects and impurities and with high carrier mobility. © *2001 MAIK "Nauka/Interperiodica"*.

INTRODUCTION

It has been reported previously [1] that Pb can be used as a neutral solvent for growing GaSb epilayers by liquid-phase epitaxy (LPE). It has been demonstrated that the use of Pb makes it possible to decrease the liquidus temperature of the system; vary the ratio between atomic fractions of Sb and Ga in the solution–melt; and decrease the concentration of native structural defects, which are characteristic of GaSb, by two orders of magnitude. As the reduced Sb concentration X^*_{Sb} increased in the liquid phase, the hole density in GaSb decreased and reached a minimum in the range X^*_{Sb} = 0.76–0.8. Here, $X^*_{Sb} = X_{Sb}/(X_{Sb} + X_{Ga})$, where X_i is the atomic fraction of the component in the liquid phase. With a further increase in the value of X^*_{Sb} in the liquid phase, new defects, whose nature is not yet clear, appeared in the epilayers. The majority-carrier mobility was highest at X^*_{Sb} = 0.6 and decreased sharply at X^*_{Sb} = 0.76–0.8. Thus, the use of Pb in growing the GaSb epilayers permitted a material with a charge-carrier density as low as $p^{(77)} = N_A - N_D = 10^{13}$ cm^{-3} at 77 K and a high degree of compensation to be obtained. This material has found wide technological application as an insulating layer.

It has been demonstrated [2, 3] that the main properties of the $Ga_{1-X}In_XAs_YSb_{1-Y}$ solid solutions ($X \le 0.22$, $Y \le 0.18$) lattice-matched to GaSb, which were obtained without using Pb, are similar to GaSb properties in many respects. Undoped layers of solid solutions, as well as GaSb epilayers, were always of *p*-type conduction. Hole density was governed by shallow-level background impurities, which were present in the starting components, and by the double-charged acceptor complex $V_{Ga}Ga_{Sb}$. The activation energy for impurity levels is E_{A1} = 0.008–0.014 eV, and those for levels of the acceptor complex were E_{A2} = 0.035 eV and E_{A3} = 0.07 eV. The shallow-level acceptor density N_{A2} decreased with an increase in X for the solid solution.

By analogy with GaSb obtained from the Pb solution–melt, it is of interest to investigate the role of Pb in growing GaSb-based quaternary $Ga_{1-X}In_XAs_YSb_{1-Y}$ solid solutions from the point of view of decreasing the structure's defect concentration and carrier density in the epilayers.

This study continues previous investigations into obtaining $Ga_{1-X}In_XAs_YSb_{1-Y}$ solid solutions from Pb-containing solution–melt [4, 5]. It is devoted to the investigation of the electrical properties of these solid solutions, the kinetics of variation in the carrier density, carrier mobility, and structure defect concentration with respect to growth conditions, as well as to the possibility of obtaining the narrow-gap solid solutions ($E_g \approx 0.4$ eV) with a high carrier mobility and low concentration of structural defects.

2. PREPARATION OF EXPERIMENTAL SAMPLES

Epilayers of the $Ga_{1-X}In_XAs_YSb_{1-Y}$ solid solutions were grown by LPE, the Pb-containing solution–melt having a cooling rate of 0.6 K/min. The *n*- and *p*-GaSb(100) single-crystal wafers were used as substrates. Binary compounds GaSb, InAs, as well as In

1063-7826/01/3508-0904$21.00

(pure to 99.999 wt %), Sb (99.999 wt %), and Pb (99.9999 wt %) were chosen as the charge components. The procedure of obtaining the epilayers was as follows. According to the thermodynamic method suggested previously [6], mole fractions of components in coexisting liquid and solid (lattice-matched to GaSb) phases were calculated for the Ga–In–As–Sb–Pb heterogeneous system. Calculations were carried out for fixed values of temperature (T) and supercooling (ΔT). Initially, the buffer p-GaSb layer with a low carrier density and high resistivity ($p = 6 \times 10^{14}$ cm^{-3} at $T = 77$ K, $\rho \gtrsim 400$ Ω cm) was grown on the n-GaSb substrate from the Pb-containing solution–melt. The buffer layer thickness was 4–5 μm. After that, based on theoretical calculation, the epilayer of the $Ga_{1-X}In_XAs_YSb_{1-Y}$ solid solution was grown on the p-GaSb buffer layer from the Pb-containing solution–melt at $T = 560$°C and supercooling $\Delta T = (3–8)$°C. The mismatch of lattice parameters for the epilayer and substrate $\Delta a/a$ was measured by double-crystal X-ray diffractometry using a TPC-1 diffractometer. The chemical composition of the solid solutions obtained was determined by qualitative X-ray spectral analysis using a JXA-5 CAMEBAX X-ray microprobe analyzer.

As a result of experiments carried out at $T = (560 \pm 3)$°C, $\Delta T = (3–8)$°C, and various Pb contents in the liquid phase, the epilayers of $Ga_{1-X}In_XAs_YSb_{1-Y}$ solid solutions ($X = 0.14–0.27$, $Y = 0.12–0.22$) lattice-matched to the GaSb(100) substrate were obtained. The growth rate, which was calculated as the ratio between the layer thickness to the growth time, was 0.3–1.0 μm/min. These values are larger than the growth rate of epilayers with the same composition, which were obtained at 560°C from the In-containing solution–melt without using Pb. According to the X-ray spectral analysis data, there was no solid-phase Pb in the samples, although the Pb content in the liquid phase was about 0.039–0.236 atomic fractions.

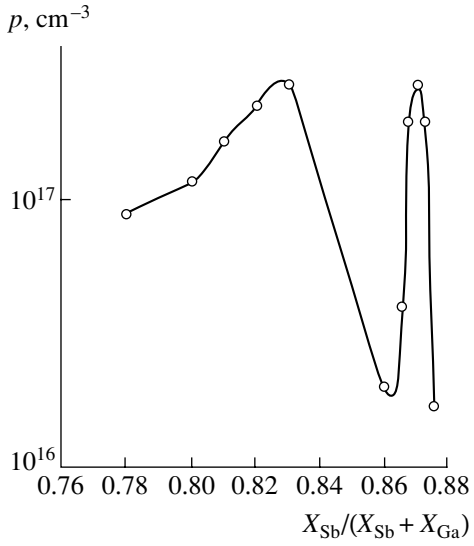

Fig. 1. Hole density p at $T = 77$ K as a function of the reduced Sb concentration $X^*_{Sb} = X_{Sb}/(X_{Sb} + X_{Ga})$.

The solid phase composition as well as the values of the band gap E_g of the $Ga_{1-X}In_XAs_YSb_{1-Y}$ solid solutions were calculated using the semiempirical formula [7] (see Table 1). As can be seen from Table 1, the experimental dependence of the In content in the solid phase on the Pb content in the liquid phase has a clearly defined maximum. Specifically, with an increase in the Pb content to 0.11 atomic fractions, the In content in the solid solution increases to $X = 0.27$. However, with a further increase in the Pb content in the liquid phase, the In content in the solid phase decreases. Such behavior of the dependence confirms the results of theoretical calculations [4, 5], which demonstrate that concentrations of solid-phase components in this system also pass through an extremum, although at other X and Y

Table 1. Dependence of the composition and band gap of the $Ga_{1-X}In_XAs_YSb_{1-Y}$ solid solutions on the Pb content in the liquid phase

Pb content in the liquid phase, atomic fractions	Composition of the $Ga_{1-X}In_XAs_YSb_{1-Y}$, atomic fractions				Band gap E_g, eV	
	calculation		experiment		$T = 300$ K	$T = 77$ K
	X	Y	X	Y		
0.2360	0.0947	0.0800	0.148	0.129	0.51	0.61
0.1951	0.1155	0.0977	0.168	0.138	0.49	0.58
0.1534	0.1417	0.1200	0.205	0.192	0.45	0.54
0.1506	0.1437	0.1217	0.210	0.160	0.44	0.53
0.1374	0.1534	0.1300	0.223	0.175	0.43	0.53
0.1229	0.1651	0.1400	0.247	0.223	0.41	0.50
0.1096	0.1768	0.1500	0.267	0.206	0.39	0.49
0.0394	0.2697	0.2300	0.194	0.148	0.46	0.55

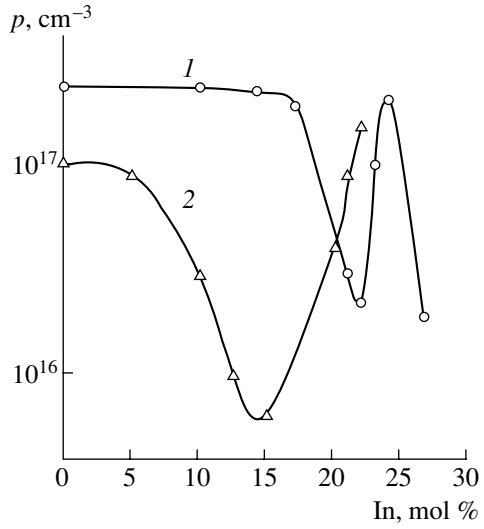

Fig. 2. Hole density p at $T = 77$ K as a function of the In content X in the GaInAsSb solid solution. Solid solutions were grown: (*1*) with the use of Pb and (*2*) without the use of Pb.

values. Previously, no epilayers more than 1 μm thick with the In content $X > 0.22$ suitable for fabricating optoelectronic devices have been obtained by LPE growth of the $Ga_{1-X}In_XAs_YSb_{1-Y}$ epilayers lattice-matched to GaSb(100) without the use of Pb. In this study, the use of Pb allowed epilayers of the $Ga_{1-X}In_XAs_YSb_{1-Y}$ solid solutions to be obtained, where $X \approx 0.27$ ($E_g \approx 0.4$ eV), see Table 1. The epilayers were 1.5–2 μm thick.

3. EXPERIMENTAL RESULTS AND DISCUSSION

The samples cut for studying galvanomagnetic effects were rectangular. On the side of the solid-solution epilayer, six In contacts were deposited and were used for measuring the electrical conductivity σ, Hall coefficient R, mobility μ, and magnetoresistance $\Delta\rho/\rho$ in a temperature range of 77–300 K. The characteristics of the samples are given in Table 2.

As can be seen from Table 2, the Hall voltage sign at $T = 77$ K for all samples (except for sample 8) is indicative of the *p*-type conduction. The dependence of the hole density at 77 K on the Sb content in the liquid phase $X^*_{Sb} = X_{Sb}/(X_{Ga} + X_{Sb})$ is shown in Fig. 1. In common with GaSb:Pb [1], a sharp decrease in the hole density with increasing X^*_{Sb} is observed. The minimum is attained at $X^*_{Sb} \approx 0.86$, which corresponds to a higher

Table 2. Characteristics of the samples investigated

Sample no.	In content (X), atomic fraction	X^*_{Sb}	$T = 300$ K			$T = 77$ K			E_{A1}, E_{A2}, E_{A3}, eV	N_{A1}, 10^{17} cm^{-3}	N_{A2}, 10^{17} cm^{-3}	N_D, 10^{16} cm^{-3}
			conduction type	n, p, 10^{17} cm^{-3}	μ, cm^2 V^{-1} s^{-1}	conduction type	n, p, 10^{17} cm^{-3}	μ, cm^2 V^{-1} s^{-1}				
1	0.120	0.777	*p*	4	500	*p*	1	1200	0.008, *A*1 0.033, *A*2	2	1.4	7
2	0.148	0.820	*p*	7	560	*p*	1.5	2200	0.008, *A*1 0.033, *A*2 0.07, *A*3	2.8	1.2	2
3	0.173	0.838	*p*	12	560	*p*	3	2300	0.01, *A*1 0.025, *A*2	4.2	3	1
4	0.210	0.862	*p*	30	80	*p*	0.46	380	0.01, *A*1 0.027, *A*2	2.3	0.5	17
5	0.223	0.858	*n*	0.3	2700	*p*	0.22	200	0.01, *A*1 0.028, *A*2	4.3	0.13	40
6	0.247	0.869	*p*	14	600	*p*	4	2700	0.008, *A*1 0.024, *A*2	4.5	0.5	5
7	0.267	0.873	*p*	5.6	530	*p*	0.18	570	0.01, *A*1 0.027, *A*2	0.48	0.2	0.6
8*	0.223	0.858	*n*	3	3900	*n*	1	4000	–	–	–	–
9*	0.247	0.869	*n*	30	2000	*p*	1.5	1400	–	–	–	–

Notes: * Denotes the Te-doped samples; $X^*_{Sb} = X_{Sb}/(X_{Sb} + X_{Ga})$; and *A*1, *A*2, and *A*3 denote the acceptor levels.

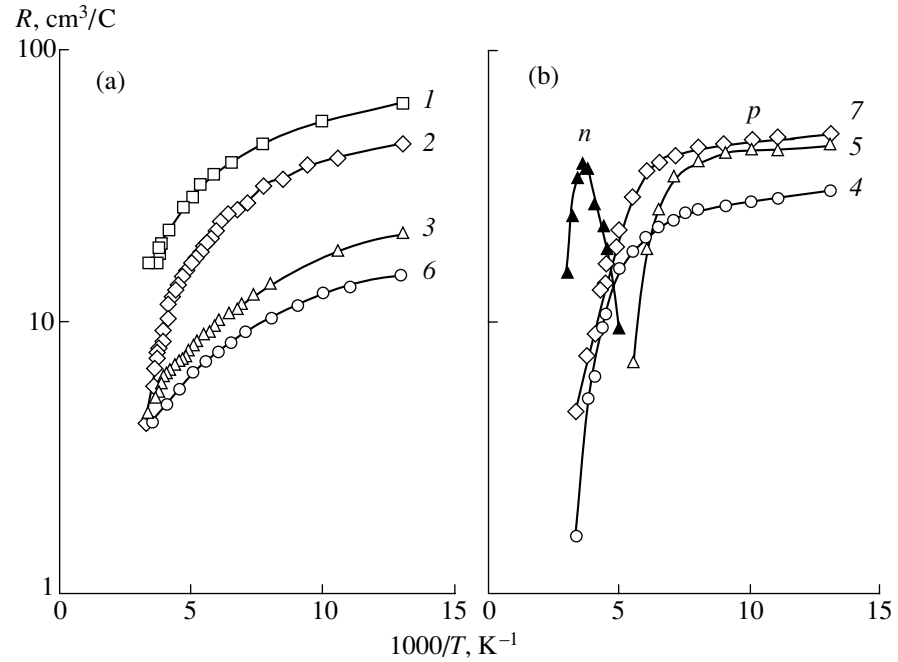

Fig. 3. Temperature dependences of the Hall coefficient R for samples with various In content X in the GaInAsSb solid solution. (a) Samples with a high mobility at $T = 77$ K and (b) samples with a low mobility at $T = 77$ K. Curve numbers correspond to sample numbers in Table 2.

Sb content in the liquid phase compared to GaSb:Pb, in which the minimum was observed at $X^*_{Sb} = 0.76$–0.8.

The dependences of the hole density on the In content in the solid solution grown in the presence of Pb (curve *1*) in comparison with solid solutions grown at the same temperatures from the same starting components without the use of Pb (curve *2*) are shown in Fig. 2. It can be seen that, if the solid solution was obtained without using Pb, the minimum of the hole density was observed at an In content of about 0.15, whereas it was impossible to obtain the solid solution for $X > 0.22$. In contrast with this, with the presence of Pb in the solution–melt, the minimum of the hole density is observed at an In content of 0.22. It is of interest that the hole density drops again at $X = 0.267$. In all cases, low mobilities correspond to low hole densities at $T = 77$ K (see Table 2).

The temperature dependences of the Hall coefficient, mobilities, and magnetic resistances for solid solutions of various compositions make it possible to investigate the energy spectrum of impurities and the mechanism of carrier scattering. The effect of Pb on the concentration and distribution of holes and structural defects for various In contents in solid solution can also be clarified.

3.1. Energy Spectrum of Impurities

The inverse-temperature dependences of the Hall coefficient for the samples listed in Table 2 are shown in Fig. 3. For the samples with a high mobility at $T = 77$ K (Fig. 3a) and with the In content $X = 0.12$–0.17 (samples 1–3), as well as for the sample with an In content of 0.247 (sample 6), shallow acceptor levels with the activation energies $E_{A1} = 0.008$–0.01 eV and deeper lying acceptor levels $E_{A2} = 0.024$–0.033 eV and $E_{A3} = 0.07$ eV are observed. The former levels are related to background impurities, which are contained in starting components of solid solutions, and the latter ones are related to the double-charged structure defect $V_{Ga}Ga_{Sb}$. For samples with a low hole density and mobility (Fig. 3b) and an In content of 0.21–0.22 (samples 4 and 5) and 0.267 (sample 7), the shallow acceptor level $E_{A1} \lesssim 0.01$ eV is also observed at $T = 77$–100 K. The deeper lying level with the activation energy $E_{A2} \approx 0.028$ eV is also observed with an increase in temperature. However, a sharp decrease in the Hall coefficient is observed for all samples at temperatures above 150 K, which points to the onset of transition to the intrinsic conductivity. For sample 7, the positive Hall voltage sign changes to a negative one at $T = 150$ K. By measuring the Hall voltage for this sample up to 400 K, we can observe that the intrinsic conductivity clearly manifests itself. However, the dependence of $RT^{3/2}$ on the inverse temperature is not exponential, and does not allow the band gap to be determined. This dependence can be explained by the pronounced compensation of impurities. For this reason, fluctuations of the potential begin to occur, and the tails of the density of states from the valence band and conduction band appear in the band gap [8].

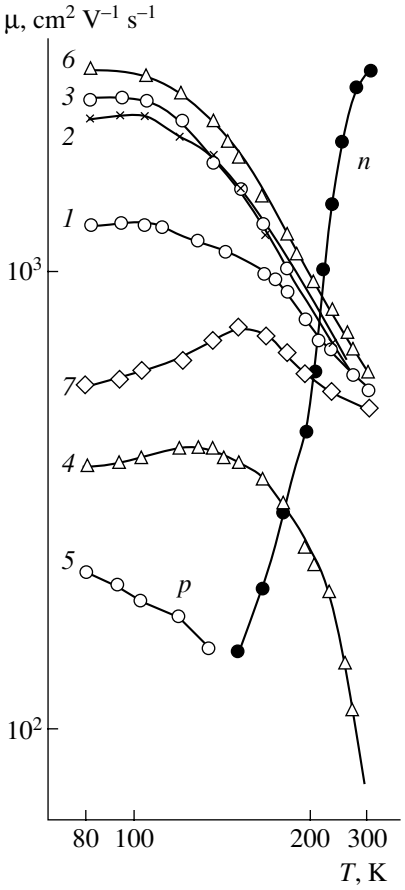

Fig. 4. Temperature dependences of mobility for samples with various In content in the solid solution. Curve numbers correspond to sample numbers in Table 2.

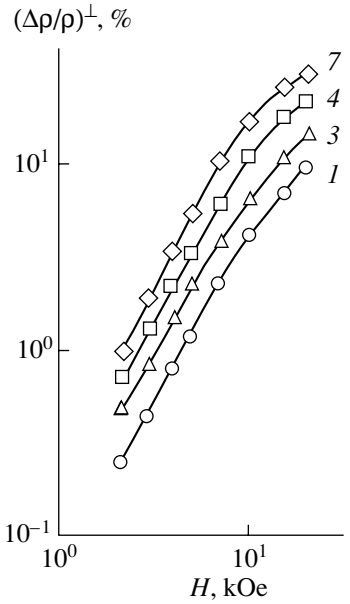

Fig. 5. Transverse magnetoresistance $(\Delta\rho/\rho)^{\perp}$ as a function of the magnetic field strength H at $T = 77$ K. Curve numbers correspond to sample numbers in Table 2.

3.2. Carrier Scattering Mechanism

Mobility μ and magnetoresistance $\Delta\rho/\rho$ are sensitive to the carrier scattering mechanism and to the type of scattering centers. The temperature dependences of mobility are shown in Fig. 4. As can be seen from Fig. 4, high mobility at 77 K is observed in the $Ga_{1-X}In_XAs_YSb_{1-Y}$ solid solutions with $X = 0.14$–0.17 and $X = 0.24$ (samples 1–3 and 6, see Table 2). At $T >$ 150 K, the mobility decreases with temperature according to the law close to $\mu \propto T^{-2}$, which is typical of lattice scattering in *p*-type III–V semiconductors [9]. At $T =$ 77–150 K, the experimental mobility μ_{exptl} is governed by scattering at impurity ions μ_I and lattice-vibration scattering μ_L

$$1/\mu_{exptl} = 1/\mu_I + 1/\mu_L. \quad (1)$$

For the samples with $X = 0.22$ and $X = 0.267$ (samples 4, 5, and 7), in which the hole density and mobility are low at $T = 77$ K, the temperature dependence of mobility at $T <$ 150–200 K points to the existence of an additional scattering mechanism apart from those involving impurity ions and lattice vibrations ($1/\mu_{exptl} = 1/\mu_I + 1/\mu_L + 1/\mu_S$). At higher temperatures, a sharp decrease in mobility is observed for these samples, whereas, in sample 5, the *p*-type conduction changes to *n*-type conduction, and the Hall mobility increases with an increase in temperature at $T >$ 150 K. In both cases, both the sharp mobility decrease and the appearance of *n*-type conduction are associated with a transition to intrinsic conductivity (appearance of electrons with a high mobility).

In order to determine the nature of the scattering centers, magnetoresistance was investigated. The transverse magnetoresistance (**I** ⊥ **H**, where **I** is the direction of a current through the sample, and **H** is the direction of the magnetic field) at $T = 77$ K is shown in Fig. 5. For all samples, the transverse magnetoresistance varies proportionally to H^2 up to 10 kOe. The coefficient $B_r^{\perp} = (\delta\rho/\rho)^{\perp}/(\mu H/c)^2$ for the samples with a high mobility (samples 1 and 3) is close to unity, which agrees with scattering by impurity ions with the participation of light and heavy holes. For the samples with a low mobility (samples 4 and 7), $B_r^{\perp} > 40$, which is well above the theoretical values calculated based on the theory of classic (Lorentzian) magnetoresistance.

For all samples, the longitudinal magnetoresistance (**I** ∥ **H**) $(\Delta\rho/\rho)^{\parallel}$ was investigated at $T = 77$ K. In this case, for the samples with a high mobility (samples 1–3 and 5), longitudinal magnetoresistance was absent. On the other hand, for all samples with a low hole mobility, longitudinal magnetoresistance was observed; however, it depended on the In content in the solid solution. It can be seen from Fig. 6 that the negative longitudinal magnetoresistance is observed for samples with an In

content of 0.21 in the solid solution (sample 4). In contrast with this, positive longitudinal magnetoresistance is observed for samples with an In content of 0.267 (sample 7).

Negative longitudinal magnetoresistance is characteristic of the quantum effect of weak localization [10]. On the other hand, so-called quantum antilocalization, or positive longitudinal magnetoresistance, is more characteristic of *p*-type Group IV and III–V semiconductors. This effect is manifested in strong spin–orbit scattering [11], which is specifically characteristic of *p*-type Group IV and III–V semiconductors. The occurrence of positive and negative magnetoresistance for the case of longitudinal magnetoresistance, in the absence of Lorentzian magnetoresistance, depends on the relationship between the frequencies of the spin–orbit scattering and phase upset for a specific sample, as in Fig. 6 at 77 K. For this interpretation, in the case of transverse magnetoresistance, large values of the coefficient $B_r^{\perp} > 40$ for samples 4 and 7 (Fig. 5) can be related to the combination of effects of quantum antilocalization (longitudinal magnetoresistance) and Lorentzian magnetoresistance.

Another explanation of the phenomena observed in the samples with low mobility also exists. Specifically, an anomalously large coefficient of the transverse magnetoresistance $B_r^{\perp}$ and appearance of the longitudinal magnetoresistance (sample 7) may be associated with clusters of impurity atoms. These clusters manifest themselves as regions distorting the paths of the current flow and bringing about the underestimation of mobility rather than as scattering centers. The effective-medium theory [12], which was developed for material with clusters of this type, yields the following formulas for mobility and magnetoresistance:

$$\mu = \mu_0(1 - 3/2)/(1 - 3/4), \quad (2)$$

$$(\Delta\rho/\rho)^{\perp} = 0.3 f(\mu_0 H/c)^2, \quad (3)$$

where μ_0 is the mobility in a homogeneous matrix, and f is the volume fraction occupied by clusters. Using the experimental data for μ and $\Delta\rho/\rho$ at $T = 77$ K and formulas (2) and (3), we determined the mobility in the matrix $\mu_0 = 4500$ cm^2 V^{-1} cm^{-1} and in the volume fraction occupied by nonuniformities $f = 0.6$.

Correlating the values of mobility μ_I at $T = 77$ K, which is determined by ion scattering and is separated out from the experimental mobility according to formula (1), with theoretical values calculated by the Brooks–Herring formula

$$\mu_I = 3.2 \times 10^{15}(m_0/m^*)^{1/2}\chi^2 T^{3/2}/N_I f(b), \quad (4)$$

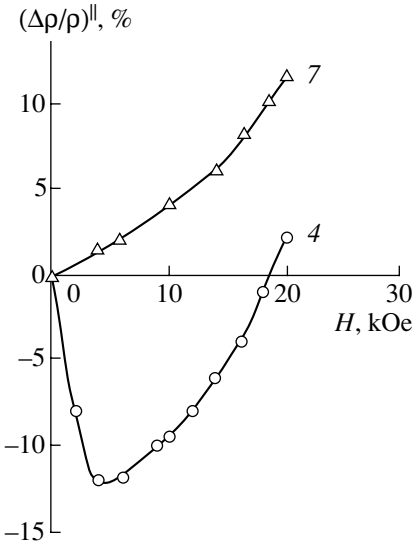

Fig. 6. Longitudinal magnetoresistance $(\Delta\rho/\rho)^{\parallel}$ as a function of the magnetic field strength H at $T = 77$ K. Curve numbers correspond to sample numbers in Table 2.

where

$$f(b) = \ln(1 + b) - b/(b + 1),$$

$$b = 1.3 \times 10^{14} T^2/p(m^*/m_0),$$

we can determine the concentration of the ionized impurity N_I (we assume that for both *p*-GaInAsSb and *p*-GaSb, the effective hole mass $m^* = 0.4m_0$, and the dielectric constant $\chi = 15.7$). For shallow impurity levels, $N_I^{(77)} = 2N_D + p^{(77)}$; thus, we can determine the acceptor concentration N_D. We determine the shallow-level acceptor concentration from the neutrality equation: $p_{\text{depl}} = N_{A1} - N_D$, where p_{depl} is the hole density corresponding to the depletion of shallow levels. We can find the concentration of the deeper lying acceptor levels N_{A2} from the concentration p at higher temperatures. The values of N_{A1}, N_{A2}, and N_D are given in Table 2.

The results obtained may be compared with the results reported previously [2, 3] for GaInAsSb solid solutions grown without using Pb. In this case, the solid solutions with the In content $X \approx 0.15$ had a low hole density and mobility and were highly compensated. In contrast with this, uncompensated material grows in the presence of Pb. For the In content $X = 0.22$, a great quantity of defects probably related to misfit dislocations was observed, whereas a highly compensated material similar to the material with an In content of 0.15, which was grown without the use of Pb, grows in the presence of Pb. Solid solutions with an In content of above 0.22 can be obtained solely in the presence of Pb in the solution–melt. In this case, solid solutions with an In content of 0.24 constituted a high-quality *p*-type uncompensated material. A great quantity of defects in

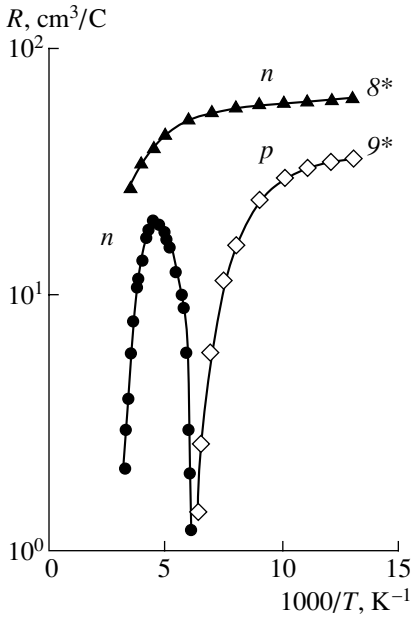

Fig. 7. Temperature dependence of the Hall coefficient for Te-doped solid solutions. Curve numbers correspond to sample numbers in Table 2.

the form of large clusters was observed in solid solutions at an In content of 0.265.

4. GaInAsSb *n*-TYPE SOLID SOLUTIONS

In order to fabricate highly efficient fast-response photodiodes for the wavelength range λ = 2.5–3 μm with low reverse currents on the basis of the $Ga_{1-X}In_XAs_YSb_{1-Y}$ solid solutions, the *n*-type epilayers with the band gap E_g = 0.4–0.5 eV are used in the device's active region. Epilayers of this type may be obtained through Te doping the solid solutions with an In content of 0.22 and 0.24.

If the starting components for growing solid solutions is not *p*-GaSb, as was described above, but *n*-GaSb:Te with the electron density $n = 5 \times 10^{17}$ cm^{-3}, the GaInSbAs solid solutions change the *p*-type conduction to *n*-type conduction. The overcompensation of the material depends on the hole density in the sample (see Table 2). With an In content in the solid solution of 0.22 (sample 5), for which the hole density is below 10^{17} cm^{-3}, complete overcompensation is observed. In this case, at T = 77 K, the material becomes *n*-type and has the electron density $n = 10^{17}$ cm^{-3} and electron mobility μ = 4000 cm^2 V^{-1} s^{-1} (see sample 8* in Table 2). A decrease in the Hall coefficient (Fig. 7, curve *8**) is observed above 200 K, which is apparently related to the onset of the transition to *p*-type conduction. With an In content in the solid solution of 0.247, for which the hole density was above 10^{17} cm^{-3} (sample 6, Table 2), with the same level of Te doping as for sample 8*, the sample is partially compensated at liquid-nitrogen temperature and preserves its *p*-type conduction (sample 9* in Table 2). However, the change of the Hall voltage sign and the transition to the intrinsic conduction occurs at T = 150 K (Fig. 7, curve *9**). The band gap E_g = 0.42 eV was determined from the slope of the $RT^{3/2}$ dependence on the inverse temperature at $T >$ 200 K, which agrees well with the value calculated (see Table 1).

5. CONCLUSIONS

In this study, the electrical properties of the $Ga_{1-X}In_XAs_YSb_{1-Y}$ solid solutions grown from the Pb-containing solution–melt on GaSb(100) substrates with an intermediate GaSb Pb-containing insulating layer were investigated for the first time. The investigations carried out allow us to make the following conclusions:

(i) The use of Pb in growing the $Ga_{1-X}In_XAs_YSb_{1-Y}$ solid solutions allowed us to obtain for the first time epilayers of these solid solutions with an In content in the solid phase X = 0.24–0.27 (E_g = 0.5–0.49 eV at T = 77 K, see Table 1) 1.5–2 μm thick, which is suitable for the development of optoelectronic devices. This was impossible without using Pb.

(ii) Undoped $Ga_{1-X}In_XAs_YSb_{1-Y}$ solid solution with the In content X = 0.22 (E_g = 0.53 eV at T = 77 K), which was obtained from the Pb-containing solution–melt, is a highly compensated material. This material is similar to a wider gap material with X = 0.15 (E_g = 0.58 eV at T = 77 K), which was obtained without using Pb.

(iii) Undoped $Ga_{1-X}In_XAs_YSb_{1-Y}$ solid solutions with the In content X = 0.247 (E_g = 0.5 eV at T = 77 K), which were obtained with the use of Pb, have low concentrations of defects and compensating impurities. They possess a high hole mobility μ = 2700 cm^2 V^{-1} s^{-1}.

(iv) Te doping of the $Ga_{1-X}In_XAs_YSb_{1-Y}$ solid solutions with the In content X = 0.22, which were obtained with the use of Pb, permits one to develop *n*-type material with a high electron mobility μ = 4000 cm^2 V^{-1} s^{-1}.

(v) The solid solutions obtained may be used to develop high-efficiency optoelectronic devices (light emitting diodes, lasers, and photodiodes) with the operating wavelength λ = 2.4–3 μm.

ACKNOWLEDGMENTS

We thank T. A. Polyanskaya, N. A. Charykov, and T. B. Popova for their help in the investigations and their participation in discussions of the results.

REFERENCES

1. A. N. Baranov, T. I. Voronina, T. S. Lagunova, *et al.*, Fiz. Tekh. Poluprovodn. (Leningrad) **23**, 780 (1989) [Sov. Phys. Semicond. **23**, 490 (1989)].
2. A. N. Baranov, A. N. Dakhno, B. E. Dzhurtanov, *et al.*, Fiz. Tekh. Poluprovodn. (Leningrad) **24**, 98 (1990) [Sov. Phys. Semicond. **24**, 59 (1990)].
3. A. N. Baranov, T. I. Voronina, A. N. Dakhno, *et al.*, Fiz. Tekh. Poluprovodn. (Leningrad) **24**, 1072 (1990) [Sov. Phys. Semicond. **24**, 676 (1990)].
4. I. A. Andreev, E. V. Kunitsyna, Yu. V. Solov'ev, *et al.*, Pis'ma Zh. Tekh. Fiz. **25** (19), 77 (1999) [Tech. Phys. Lett. **25**, 792 (1999)].
5. E. A. Kunitsyna, I. A. Andreev, N. A. Charykov, *et al.*, Appl. Surf. Sci. **142**, 371 (1999).
6. A. M. Litvak and N. A. Charykov, Zh. Khim. Fiz. **64**, 2331 (1990).
7. T. C. DeWinter, M. A. Pollack, A. K. Strivastava, and J. I. Zuskind, J. Electron. Mater. **4**, 729 (1985).
8. B. I. Shklovskiĭ and A. L. Efros, *Electronic Properties of Doped Semiconductors* (Nauka, Moscow, 1979; Springer-Verlag, New York, 1984).
9. D. Kranzer, Phys. Status Solidi A **26**, 11 (1974).
10. A. Kawabata, J. Phys. Soc. Jpn. **42** (2), 628 (1980).
11. B. L. Al'tshuler, A. G. Aronov, A. I. Larkin, and D. E. Khmel'nitskiĭ, Zh. Éksp. Teor. Fiz. **81**, 768 (1981) [Sov. Phys. JETP **54**, 411 (1981)].
12. M. H. Cohen, Phys. Rev. Lett. **30**, 698 (1973).

Translated by N. Korovin